

General Disclaimer

One or more of the Following Statements may affect this Document

- This document has been reproduced from the best copy furnished by the organizational source. It is being released in the interest of making available as much information as possible.
- This document may contain data, which exceeds the sheet parameters. It was furnished in this condition by the organizational source and is the best copy available.
- This document may contain tone-on-tone or color graphs, charts and/or pictures, which have been reproduced in black and white.
- This document is paginated as submitted by the original source.
- Portions of this document are not fully legible due to the historical nature of some of the material. However, it is the best reproduction available from the original submission.

X-620-77-151

PREPRINT

TMX-71355

**SCALING OF CROSS SECTIONS
FOR K-ELECTRON CAPTURE BY
HIGH-ENERGY PROTONS AND
ALPHA-PARTICLES FROM
THE MULTIELECTRON ATOMS**

(NASA-TM-71355) SCALING OF CROSS SECTIONS
FOR K-ELECTRON CAPTURE BY HIGH-ENERGY
PROTONS AND ALPHA-PARTICLES FROM THE
MULTIELECTRON ATOMS (NASA) 27 p
HC A03/MF A01

N77-28924

Unclas
39024

CSSL 20H G3/72

K. OMIDVAR

JUNE 1977



**— GODDARD SPACE FLIGHT CENTER —
GREENBELT, MARYLAND**

SCALING OF CROSS SECTIONS FOR K-ELECTRON CAPTURE BY
HIGH-ENERGY PROTONS AND ALPHA-PARTICLES FROM THE MULTIELECTRON ATOMS

K. Omidyar
Stratosphere Physics and Chemistry Branch
Laboratory for Planetary Atmospheres
NASA/Goddard Space Flight Center
Greenbelt, Maryland 20771

ABSTRACT

Electron capture by protons from H, He, and the K-shell of Ar, and alpha particles from He are considered. It is shown that when certain function of the experimental cross sections is plotted versus the inverse of the collision energy, at high energies the function falls on a straight line. At lower energies the function concaves up or down, depending on the charge of the projectile, the effective charge and the ionization potential of the electron that is being captured. The plot can be used to predict cross sections where experimental data are not available, and as a guide in future experiments. High energy scaling formulas for K-electron capture by low-charge projectiles are given.

I. INTRODUCTION

It is well known that an approximation developed by Oppenheimer,¹ and Brinkman and Kramers² for electron capture by protons from the multi-electron atoms results in cross sections that when plotted as functions of the collision energy would give curves similar in shape to the experimental curves, but are larger by as much as an order of magnitude.³ This indicates that in the region of validity of the approximation the calculated cross section in some respects has the correct functional form of the actual cross section.

In this paper this approximation is used to calculate the K-electron capture by protons and alpha-particles from the multi-electron atoms with the assumption of the hydrogenic wave functions with effective charges for the K-shell electrons. A feature in the present calculation which usually is absent in other calculations is to use the measured ionization potential of the K-shell instead of the hydrogenic ionization potential which is proportional to the square of the effective charge. This choice to some extent compensates for the unphysical assumption that the target potential is coulombic, and the neglect of the readjustment of the parent ion when the capture takes place. Nikolaev³ has also introduced the actual, instead of the hydrogenic, ionization potential. However, his final results do not seem to be the same as those presented here.

Using the above prescription, the prior and post forms of the cross section, and their asymptotic forms with respect to energy are given analytically. Based on the asymptotic forms, a plot of a function of the cross section versus the inverse of the energy is given where at

moderately high energies, when $E_p \gg M_p Z_{\text{eff}}^2$, the experimental data falls on a straight line. E_p and M_p are the energy and mass of the projectile in rydberg and electron mass units, and Z_{eff} is the effective charge of the target. For lower energies the lines concave up or concave down, depending on the charge of the projectile, the effective charge and the ionization potential of the K-shell.

It is shown that these features are satisfied using the experimental data for electron capture by protons from H, He, and the K-shell of Ar, and for electron capture by α -particles from He.

A scaling law that connects different charge exchange cross sections to the $p + H$ charge transfer is presented. Also, a formula with two arbitrary parameters that are fitted to the experimental data for the K-shell electron capture cross section is given that can be used for different charge transfer reactions provided the projectile charge is not too large. For energies $E_p \geq 2 M_p Z_{\text{eff}}^2$ the cross sections derived by this formula are within a factor of 2 of the experimental data mentioned before.

For energies larger than 100 MeV/nucleon, the asymptotic form of the capture cross section is governed by the second Born approximation⁴ which is different from the asymptotic form according to the first Born, and the simple formula derived here is invalid in this energy region. This energy region at present is beyond the interest of the experimenters.

II. FORMULATION

We consider capture of a K-shell electron by a proton or a structureless ion from a multielectron atom. The squared of the prior and post forms of the exchange amplitude in the Oppenheimer-Brinkman-Kramers, from here on called OBK, approximation and the assumption that the K-electrons can be described by hydrogenic wave functions are given by⁵

$$|T_{(i, f)}^{P_r}|^2 = \frac{2^{10} \pi^2 a_0^2 e^4 m_i^2 (d_1 d_2)^5}{(d_2^2 + B^2)^4 (d_1^2 + C^2)^2} \quad (1)$$

$$|T_{(i, f)}^{P_0}|^2 = \frac{2^{10} \pi^2 a_0^2 e^4 m_i^2 (d_1 d_2)^5}{(d_2^2 + B^2)^2 (d_1^2 + C^2)^4} \quad (2)$$

$$d_1 = \frac{\mu_{13} Z_p}{m_e a_0 n_1}, \quad d_2 = \frac{\mu_{23} Z_{eff}}{m_e a_0} \quad (3)$$

$$\vec{B} = \frac{\mu_{23}}{m_e} \vec{k}_1 - \vec{k}_2, \quad \vec{C} = \vec{k}_1 - \frac{\mu_{13}}{m_e} \vec{k}_2 \quad (4)$$

In these equations n_1 is the principal quantum number of the electron after capture, μ_{13} and μ_{23} are the reduced masses of the projectile + electron and target nucleus + electrons, and Z_p and Z_{eff} are the projectile's charge and the effective charge of the K-shell electron in units of the absolute value of the electronic charge e . m_e is the electron mass, and a_0 is the Bohr's radius. \vec{k}_1 and \vec{k}_2 are the center of mass propagation vectors before and after collision. The magnitudes of k_1

and k_2 are related through the conservation of energy by

$$\frac{\hbar^2 k_2^2}{2\mu_2} = \frac{\hbar^2 k_1^2}{2\mu_1} - I(2,3) + I(1,3) \quad (5)$$

where μ_1 and μ_2 are the reduced masses of the system before and after collision and $I(2,3)$ and $I(1,3)$ are the ionization potentials of the transferred electron before and after collision.

The cross section is then expressed through

$$\sigma = \frac{\mu_1 \mu_2 \hbar^2}{4\pi^2 \hbar^4 k_1} \int |T(i, f)|^2 d(\hat{k}_1 \cdot \hat{k}_2) \quad (6)$$

where $\hat{k}_1 \cdot \hat{k}_2 = \cos \theta$ with θ the scattering angle.

It can be shown that most contribution to the cross section comes from scattering angles θ of the order m_e/M , where M is the proton mass. Then neglecting terms of the order m_e/M we obtain⁶

$$a_0^2 (d_2^2 + B^2) = Z_{eff}^2 + \frac{U^2}{4} \left[\left(1 - \frac{\Delta I}{U^2}\right)^2 + g^2 \left(\frac{2bc}{b+c}\right)^2 \right] \quad (7)$$

$$a_0^2 (d_1^2 + c^2) = Z_P^2 / m_i^2 + \frac{U^2}{4} \left[\left(1 + \frac{\Delta I}{U^2}\right)^2 + g^2 \left(\frac{2bc}{b+c}\right)^2 \right] \quad (8)$$

$$g = (M/m_e) \theta, \quad U = v_1 / v_0 \quad (9)$$

In the above v_1 is the initial relative velocity of the colliding particles, and v_0 is the Bohr's velocity. b and c are defined such that bM and cM are the incident particle and target nucleus masses. ΔI is the initial minus the final ionization potentials of the transferred electron in rydberg.

The actual ionization potential of the K-electron is less than Z_{eff}^2 Ryd due to the repulsion of the electrons outside the K-shell when a K-electron is being removed to infinity. Let this difference be δ .

Then

$$\delta = Z_{\text{eff}}^2 - Z_p^2 / n_i^2 - \Delta I \quad (10)$$

By subtracting (7) from (6) we obtain

$$\delta = a_0^2 [(a_2^2 + B^2) - (a_1^2 + C^2)] \quad (11)$$

To carry out the integration in (6) we introduce $y = (2bc/(b+c))^2 g^2$. Keeping in mind that the main contribution to the integral in (6) comes from small values of θ , by combining (7), (8), (1) and (6) we obtain for the prior form

$$\sigma_{(i,f)}^{Pr} = \frac{2^8}{3} \pi a_0^2 n_i^2 (a_0^2 a_1 a_2)^5 \frac{\delta^4}{\delta (a_0^2 a_2^2)^3 \delta (a_0^2 a_1^2)} \int_0^{\infty} \frac{dy}{(P + \frac{U^2}{4} y)(Q + \frac{U^2}{4} y)} \quad (12)$$

$$P = a_0^2 a_2^2 + \frac{U^2}{4} \left(1 - \frac{\Delta I}{U^2}\right)^2, \quad Q = a_0^2 a_1^2 + \frac{U^2}{4} \left(1 + \frac{\Delta I}{U^2}\right)^2 \quad (13)$$

in the derivation of (12) we have also assumed that $k_2/k_1 \approx 1$. Since μ_2 differs from μ_1 by terms of the order m_e/M , Eq. (5) shows that the above assumption is justified when the incident energy is much larger than the difference in the binding energies. The expression for σ in (13) is a

factor of 2 larger than the expression for σ in (6), since we have assumed 2 electrons for the K-shell.

Evaluation of the integral in (12) results in

$$\sigma_{(i, f)}^{Pr} = \frac{9 \pi a_0^2}{m^3} \frac{Z_P^5}{Z_{eff}^7} \frac{1}{s^2 P^5} \sum_{l=0}^{\infty} \frac{l+1}{l+5} \left(\frac{\delta_0}{P} \right)^{4l} \quad (14)$$

$$s = \frac{v}{Z_{eff} v_0}, \quad \delta_0 = \frac{\delta}{Z_{eff}^2}, \quad P = 1 + \frac{s^2}{4} \left(1 - \frac{\Delta I_0}{s^2} \right)^2, \quad \Delta I_0 = \frac{\Delta I}{Z_{eff}^2} \quad (15)$$

where s is the incident velocity in units of the average orbital velocity of the K-electrons. With the help of (15) and (10) it can be shown without any difficulty that $p > \delta_0$ always. Then the series in (14) always converges.

Similar to the derivation of (14), the following expression can be derived for the post-form of the cross section:

$$\sigma_{(i, f)}^{Po} = \frac{9 \pi a_0^2}{m^3} \frac{Z_P^5}{Z_{eff}^7} \frac{1}{s^2 (P - \delta_0)^5} \sum_{l=0}^{\infty} \frac{l+1}{l+5} \left(\frac{-\delta_0}{P - \delta_0} \right)^{4l} \quad (16)$$

The series converges in all practical cases. By letting $\delta_0 = \delta/Z_{eff} \rightarrow 0$ in (14) and (16), which amounts to assuming hydrogenic potential for the K-shell, the prior and post forms of the cross section reduce to the familiar form of the OBK cross section with the assumption of the hydrogenic potential⁶

$$\sigma_{(i, f)}^H = \frac{19 \pi a_0^2}{5 m^3} \frac{Z_P^5 Z_{eff}^{-7} s^8}{\left[s^4 + 2(Z_{eff}^2 + Z_P^2/m^2) s^2 + (Z_{eff}^2 - Z_P^2/m^2)^2 \right]^5} \quad (17)$$

Since we are dealing with high energy approximation, it is appropriate to have the cross section in terms of the inverse powers of s^2 . Let us introduce $x = 1/s^2$, then (14) can be written in the following form:

$$\left[\frac{n_i^3 Z_{eff}^7 s^{12} \sigma^P(\pi a_0^2)}{2^{19} Z_P^5} \right]^{-1/5} = \frac{1 + 2(2 - \Delta I_0)x + (\Delta I_0)^2 x^2}{\left[\sum_{l=0}^{\infty} \frac{l+1}{l+5} \left(\frac{\delta_0}{P} \right)^l \right]^{1/5}} \quad (18)$$

Making use of the definition of p , the right hand side can be expanded in powers of x . In this way we obtain to terms of the order x^2 :

$$\left[\frac{5n_i^3 Z_{eff}^7 s^{12} \sigma^P(\pi a_0^2)}{2^{19} Z_P^5} \right]^{-1/5} \approx 1 + 2\left(2 - \Delta I_0 - \frac{2}{3}\delta_0\right)x - \left(\frac{32}{21}\delta_0^2 - (\Delta I_0)^2\right)x^2, \quad x = s^{-2} \ll 1 \quad (19)$$

Similarly, for the post-form of the cross section we obtain up to x^2 :

$$\left[\frac{5n_i^3 Z_{eff}^7 s^{12} \sigma^P(\pi a_0^2)}{2^{19} Z_P^5} \right]^{-1/5} \approx 1 + 2\left(2 - \Delta I_0 - \frac{4}{3}\delta_0\right)x - \left(\frac{32}{21}\delta_0^2 - (\Delta I_0)^2\right)x^2, \quad x = s^{-2} \ll 1 \quad (20)$$

The two expressions have the same dependence with respect to x^2 , but they are different in their dependence on x .

Equation (17) can also be written in a form similar to (19) or (20):

$$\left[\frac{5n_i^3 Z_{eff}^7 s^{12} \sigma^H(\pi a_0^2)}{2^{19} Z_P^5} \right]^{-1/5} = 1 + 2\left(1 + \frac{Z_P^2}{n_i^2 Z_{eff}^2}\right)x + \left(1 - \frac{Z_P^2}{n_i^2 Z_{eff}^2}\right)^2 x^2 \quad (21)$$

For the resonance $H^+ + H$ charge exchange collisions, where $\Delta I_0 = \delta_0 = 0$, and $Z_p = Z_{\text{eff}} = 1$, the right hand sides of (19) through (21) become $1 + 4x$, and the three forms of the cross sections become the same.

The forms of Eqs. (19) - (21) suggest that if the left hand sides of these equations are plotted versus x , for $x \ll 1$ a straight line is obtained. In the next section we will show that this linearity is satisfied by the experimental data.

Similarly, Eqs. (19) and (20) suggest that if we plot the left hand sides of these equations versus x , for the resonance $H^+ + H$ charge exchange collisions we should obtain a straight line, while for non-resonance charge transfers the plot should be concave up or down, depending on the values of Z_p , Z_{eff} , and the K-shell ionization potentials. In the next section this aspect of the theory will also be tested against the experimental data.

II. RESULTS AND DISCUSSIONS

Assuming relationships (19) and (20) are followed experimentally, for $s^2 \gg 1$ the quantity $Z_{\text{eff}}^7 \sigma(\pi a_0^2) / Z_p^5$ becomes a function of s^2 only, and if this quantity is plotted versus s^2 , all the experimental points should fall on a single curve. To see to what extent this scaling law is obeyed at low energies and how the scaling law is approached as s^2 increases, in Figure 1 the product $Z_{\text{eff}}^7 \sigma(\pi a_0^2)$ for low energy electron capture by protons from atomic hydrogen, helium, and the K-shell of argon are plotted versus s^2 .

As is seen in the figure the agreement among the three curves improves as the energy increases. At the positions of the maxima for the He and Ar curves, the ordinate of the Ar curve is about twice the He curve, and about 4 times of the H curve. The corresponding cross sections in this region are many orders of magnitudes different from each other. For example at $s^2 = 0.4$ corresponding to 10 keV protons on H the measured cross section is 10^{-15} cm^2 (Ref. 6), at $s^2 = 0.42$ corresponding to 30 keV protons on He the measured cross section is $1.9 \times 10^{-16} \text{ cm}^2$ (Ref. 7), and at $s^2 = 0.351$ corresponding to 3 MeV protons on Ar K-shell, the experimental cross section is $2.72 \times 10^{-23} \text{ cm}^2$ (Ref. 8). Due to the large variation of different cross sections, the agreement obtained in Figure 1 is impressive.

No scaling here is made for the dependence of the charge-exchange cross section on Z_p . A low velocity calculation by Olson and Salop¹⁰ indicate that for high Z_p the cross section increases approximately linearly with respect to Z_p , while a Z_p^2 dependence is predicted by Presnyakov and Uiantsev.¹¹ The classical binary encounter method¹² also gives a Z_p^2 dependence.

Using the measured cross sections for 4 different charge-exchange processes, in Figure 2, the left hand sides of (19) or (20), except for a numerical factor, are plotted versus $x = 1/s^2$. According to these equations, for $x \ll 1$ the experimental points should fall on a straight line. As x increases these points should concave up or down, depending on the values of Z_p , Z_{eff} and the target's ionization potential.

As is seen the linearity for small x is satisfied to a good degree, specially for p + H and p + He points. As x becomes larger,

the data for $p + H$ continue to fall on a straight line, as predicted by (19) and (20), while the data for $p + He$ concave down, and those for $He^{++} + He$ concave up, in accord with the calculation as will be explained below. There are not enough data for $P + Ar$ for low x to make a judgment. Four of the five experimental points for this case lie on a straight line that passes, presumably accidentally, through the y -axis at the common point that theoretically all charge transfer cross sections should pass through.

Using the values of Z_p , Z_{eff} , and the K-shell ionization potentials for the 3 non-hydrogenic target cases, we find that the right hand sides of (19) and (20) are given by

$$\begin{array}{ll}
 1 + 2.95 x - 0.122 x^2 & \text{Prior} \\
 1 + 2.46 x - 0.122 x^2 & \text{Post}
 \end{array}
 \left. \vphantom{\begin{array}{l} \text{Prior} \\ \text{Post} \end{array}} \right\} p + H_e$$

$$\begin{array}{ll}
 1 + 5.05 x + 0.389 x^2 & \text{Prior} \\
 1 + 4.56 x + 0.389 x^2 & \text{Post}
 \end{array}
 \left. \vphantom{\begin{array}{l} \text{Prior} \\ \text{Post} \end{array}} \right\} He^{++} + H_e$$

$$\begin{array}{ll}
 1 + 2.16 x + 0.521 x^2 & \text{Prior} \\
 1 + 1.86 x + 0.521 x^2 & \text{Post}
 \end{array}
 \left. \vphantom{\begin{array}{l} \text{Prior} \\ \text{Post} \end{array}} \right\} p + Ar$$

Then for $p + H_e$ and $He^{++} + H_e$ cases we find agreement with measurements as far as convexity and concavity are concerned. For $p + Ar$ case where not enough data is available, the theory predicts that the data should concave up.

It is of interest to note that the curve obtained by using the hydrogenic potential for the cross section, Eq. (21), always concaves up, contrary to the experimental data.

Suppose a projectile of mass M_p , charge Z_p , and energy E_p captures an electron from a target of effective charge Z_{eff} . Then for $x \ll 1$, or

$E_p/M_p Z_{eff}^2 \gg 1$, with E_p and M_p in units defined before, the cross section $\sigma_{Z_p, Z_{eff}}(E_p)$ according to (19) - (21) is related to the cross section for electron capture by protons from H at energy E_0 , $\sigma_{1,1}(E_0)$, by

$$\sigma_{Z_p, Z_{eff}}(E_p) \approx g \frac{Z_p^5}{Z_{eff}^7} \sigma_{1,1}(E_0), \quad E_0 = \frac{M E_p}{M_p Z_{eff}^2} \quad (22)$$

where g is the number of electrons in the target K-shell, and M is the proton's mass. The condition $x \ll 1$ makes this formula inapplicable to many cases of interest. The formula can be used as an estimate of the cross section when the data fall approximately on each other.

As an example, from the graph of Gilbody and Ryding¹⁴ the $p + H$ cross section at 130 keV is about $0.048 \pi a_0^2$. Using this value and the scaling (22), we find that the cross section for the $He^{++} + He$ case at 1.50 MeV is $0.079 \pi a_0^2$. From the graph of Pivovar et al.¹⁷ the cross section for H_e^{++} on He is about 0.055, which is 30% smaller than the value predicted by (22).

An alternative way of finding a general formula for the charge-exchange cross section is to assume that the right-hand sides of (19) and (20) are a polynomial in x , and to find the coefficients of the polynomials by least square fitting to the data. This has been done for a polynomial up to two terms. The corresponding cross section is given by

$$\sigma(\text{Scaled}) = \frac{2^{19} \pi a_0^2}{5} \frac{Z_p^5}{Z_{eff}^7} \frac{x^6}{(b_0 + b_1 x)^5},$$

$$x = \frac{M_p Z_{eff}^2}{E_p} \ll 0.5, \quad b_0 = 1.073, \quad b_1 = 6.23 \quad (23)$$

where for determination of b_0 and b_1 we have considered all the data given in Figure 2 in the range $0 \leq x \leq 0.50$.

The ratio of the experimental cross section to σ (scaled) is plotted in Figure 3. This ratio in the figure ranges between 0.60 to 1.80. We conclude that for energies E_p such that $E_p \geq 2 M_p Z_{\text{eff}}^2$, formula (23) gives the experimental cross sections within a factor of 2.

In Figures 4 through 7 the data points of Figure 2 for each process are redrawn, and are compared with the prior and post forms of the OBK cross sections as given by (14) through (16). In the case of the $p + H$ the prior and post forms are given by a single curve.

For the non-hydrogenic targets, the two forms come together at high energies, but for the low energies, the prior form agrees always better with the measurements. The fact that the post form is a bad approximation can be seen physically as follows:

In the post form the interaction which causes the transition is between the captured electron and its parent ion. The parent ion is assumed to be a point charge in the post form while in reality this ion has a structure different from a point charge. This difficulty does not arise in the prior form.

Another difficulty with the post form is that when the projectile is a multiply charged ion, there is a coulomb interaction between the particles in the final state, while in the post form the relative motion of these particles is described by a plane wave. However, it has been shown by Bates and Boyd¹⁸ that for energies in the keV region or larger the effect of the coulomb repulsion between the particles can be neglected.

From Figures 4-7 it can be seen that as the energy increases, the discrepancy between the experimental and OBK cross sections decreases. As an example, it can be determined from Fig. 4 that for the p + H case the ratio of the OBK to the experimental cross section decreases from 5.9 at 50 keV energy to 4.2 at 130 keV. In the p + He case, Fig. 5, this ratio changes from 4.3 at 200 keV to 2.2 at 10.5 MeV. This decrease in the ratio has also been noted by Nikolaev³ and Halpern and Law.¹⁹ Based on Fig. 5 we can conclude that this ratio never reaches unity.

Nikolaev introduces an energy dependent empirical factor which is defined as the ratio of the experimental to the OBK cross sections for electron capture from all shells of the multielectron atoms. This ratio is obtained by fitting the OBK approximation to the experimental data. It approaches zero for energies very small and very large, and reaches a maximum of 0.455 for $v/(\sqrt{Z_{\text{eff}}} v_0) \approx 1.62$. Despite its usefulness, the main difficulty with this factor is that in the energy region of interest the ratio of the experimental to the OBK cross sections increases as the energy increases, but this factor decreases with increasing energy.

In the present paper we have considered protons and alpha-particles as projectiles. It is also of interest to consider the heavier bare nuclei. The present scaling is not applicable to the heavier nuclei due to the fact that for these nuclei electrons are captured predominantly in many excited states, while the present treatment considers capture into a single state, namely the ground state.

The quantum number n_1 for which the capture cross section is maximum can be obtained by minimizing the product of the left hand side of (21) and $n_1^{-3/5}$ with respect to n_1 . In this way we find that the cross section

becomes maximum for a value of n_1 such that

$$n_1 = \left\{ \frac{7}{3} \frac{s^2 - 1}{(s^2 + 1)^2} \left[1 + \sqrt{1 + \frac{51}{49} \left(\frac{s^2 + 1}{s^2 - 1} \right)^2} \right] \right\}^{1/2} \frac{Z_p}{Z_{eff}} \quad (24)$$

Then the value of n_1 for which the cross section becomes maximum is directly proportional to Z_p . For $s^2 \gg 1$ we obtain

$$n_1 \approx 2.38 \frac{Z_p v_0}{v_1}, \quad s^2 \gg 1 \quad (25)$$

As an example, for a F_e^{+26} projectile of 10 MeV/nucleon energy corresponding to $v_1/v_0 \approx 20$ incident on atomic hydrogen the maximum cross section occurs at $n_1 = 3$. Capture cross section into the ground state will not dominate until the energy is well above 100 MeV/nucleon.

IV. CONCLUSION

It is shown that the cross section according to the OBK approximation represent correctly some aspect of the functional dependence of the available experimental cross sections on the collision energy. A plot of a function of the available experimental cross sections can be used to predict cross sections where experimental data are not available, and as a guide for future experiments. Some scaling formulas are given.

REFERENCES

1. J. R. Oppenheimer, Phys. Rev. 31, 349 (1928).
2. H. C. Brinkman and H. A. Kramers, Proc. K. Ned. Akad. Wet. 33, 973, (1930).
3. V. S. Nikolaev, Zh. Eksp. Teor. Fiz. 51, 1263 (1966) [Sov. Phys. - JETP 24, 847 (1967)].
4. P. J. Kramer, Phys. Rev. A 6, 2125 (1972), and the references thereof.
5. J. D. Jackson and H. Schiff, Phys. Rev. 89, 359 (1953).
6. H. Schiff, Can. J. Phys. 32, 393 (1954).
7. R. F. Stebbings, A. C. H. Smith, and W. L. Fite, Proc. Roy. Soc. A 268, 527 (1962).
8. S. K. Allison, Rev. Mod. Phys. 30, 1137 (1958).
9. J. R. Macdonald, C. L. Cocke, and W. W. Eidson, Phys. Rev. Lett. 32, 648 (1974).
10. R. E. Olson and A. Salop, Phys. Rev. A 14, 579 (1976).
11. L. P. Presnyakov and A. D. Ulantsev, Kvant. Elektron 1, 2377 (1974) [Sov. J. Quantum Electron 4, 1320 (1975)].
12. J. D. Garcia, E. Gerjuoy, and J. E. Welker, Phys. Rev. 165, 72 (1968).
13. W. L. Fite, R. F. Stebbings, D. G. Hummer, and R. T. Brackman, Phys. Rev. 119, 663 (1960).
14. H. B. Gilbody and G. Ryding, Proc. Roy. Soc. A 291, 438 (1966).
15. L. M. Welsh, K. H. Berkner, S. N. Kaplan, and R. V. Pyke, Phys. Rev. 158, 85 (1967).
16. K. H. Berkner, S. N. Kaplan, G. A. Paulikas, and R. V. Pyke, Phys. Rev. 140, A729 (1967).

- O. J.
O. P.
17. L. I. Pivovarov, M. T. Novikov, and V. M. Tubaev, Zh. Eksp. Teor. Fiz. 42, 1490 (1962) [Sov. Phys. - JETP 15, 1035 (1962)].
 18. D. R. Bates and A. H. Boyd, Proc. Phys. Soc. 80, 1301 (1962).
 19. A. M. Halpern and J. Law, Phys. Rev. Lett. 31, 4 (1973).

FIGURE CAPTIONS

Figure 1. A plot of $Z_{\text{eff}}^7 \sigma(\pi a_0^2)$ versus $v^2/(Z_{\text{eff}} v_0)^2$ for electron capture by protons from H (Ref. 7), He (Ref. 8), and K-shell of Ar (Ref. 9). The effective charges for He and K-shell of Ar are assumed to be 1.69 and 17.4. Since there is one K-shell electron for H instead of 2, for uniform scaling the corresponding cross section has been multiplied by 2. The positions on the abscissa where the cross section according to the OBK approximation become maximum for He and Ar targets are indicated by arrows. They can be compared to the positions of the experimental maxima.

Figure 2. A plot of $Z_p Z_{\text{eff}} [v/v_0]^{12} \sigma(\pi a_0^2)]^{-1/5}$ versus $(Z_{\text{eff}} v_0)^2/v^2$ for single electron capture in the following processes: i) Proton on H (Fite et al. (Ref. 13) and Gilbody et al. (Ref. 14)). ii) Proton on H_e (Allison et al. (Ref. 8), Welsh et al. (Ref. 15), and Berkner et al. (Ref. 16)). iii) Proton on Ar (K-shell, McDonald et al. (Ref. 9)). iv) Alpha-particles on H_e (Pivovar et al. (Ref. 17)).

Figure 3. A plot of the ratio of the experimental to the scaled, Eq. (23), cross sections versus $(v_0 Z_{\text{eff}})^2/v^2$. The ratio for each experimental point is designated by the sign of the experimental point used in Figure 2.

- Figure 4. Comparison between the experimental data for $H^+ + H$ charge exchange of Gilbody and Ryding (Ref. 14) and the OBK cross section. In this and the following three figures the abscissas and ordinates are the same as in Figure 2.
- Figure 5. Comparison between the experimental data for electron capture by proton from H_e and the prior and post forms of the OBK cross section.
- Figure 6. Comparison between the experimental data for electron capture by protons from the K-shell of Ar (Macdonald et al. (Ref. 9)) and the prior and post forms of the OBK cross section.
- Figure 7. Comparison between the experimental data for electron capture by He^{++} from H_e (Pivovar et al. (Ref. 17)) and the prior and post forms of the OBK cross section.

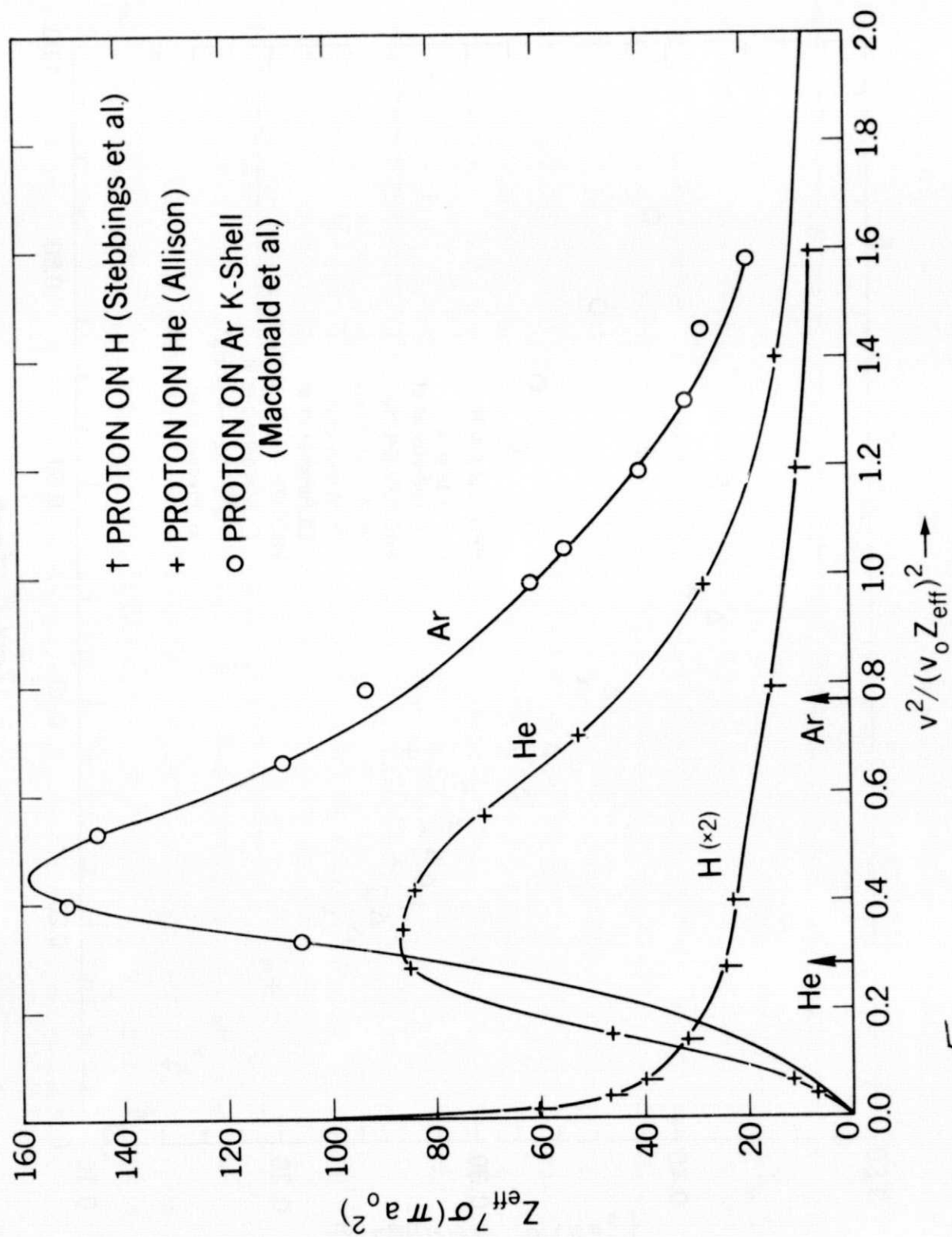


Figure 1

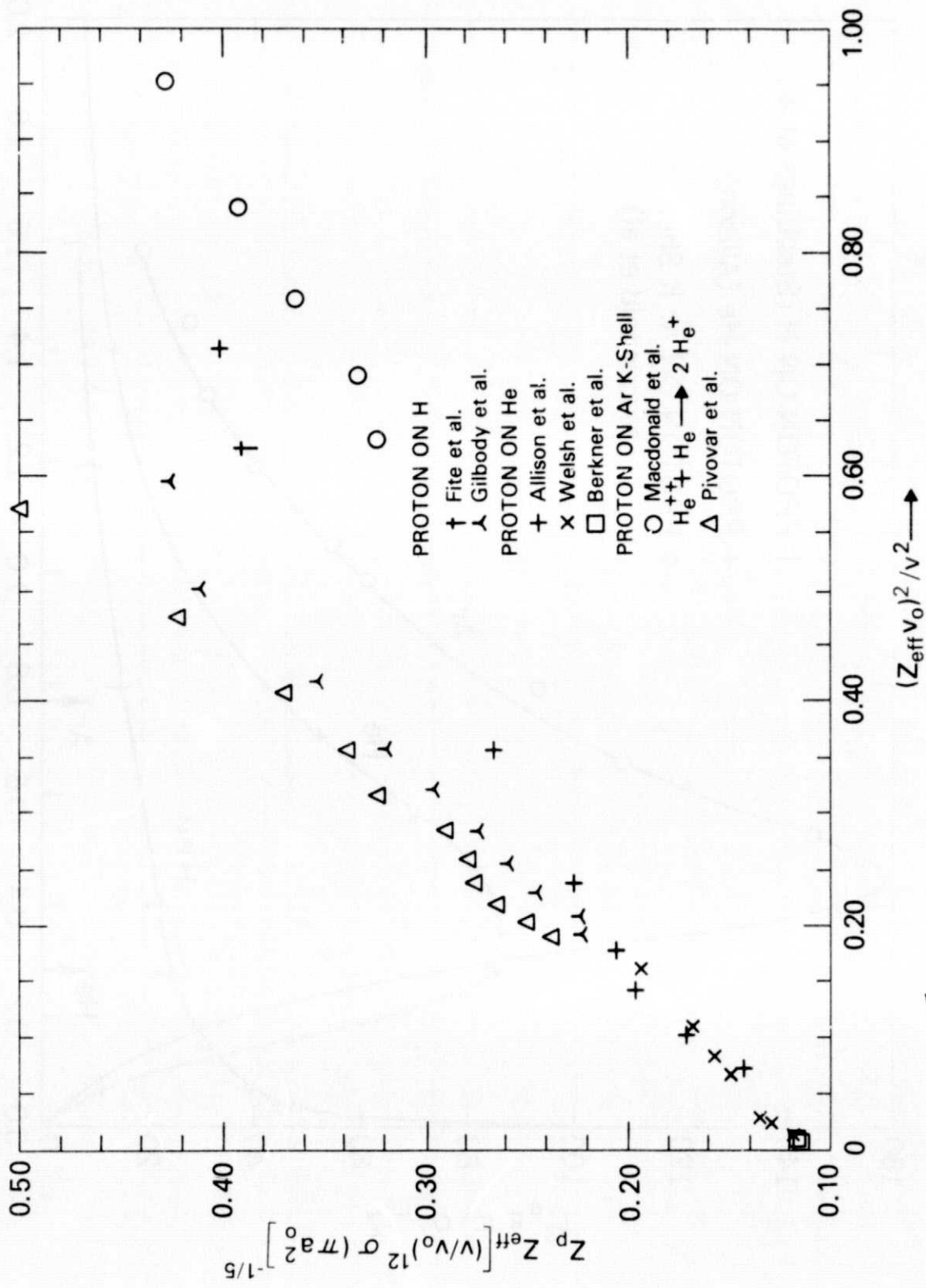


Figure 2

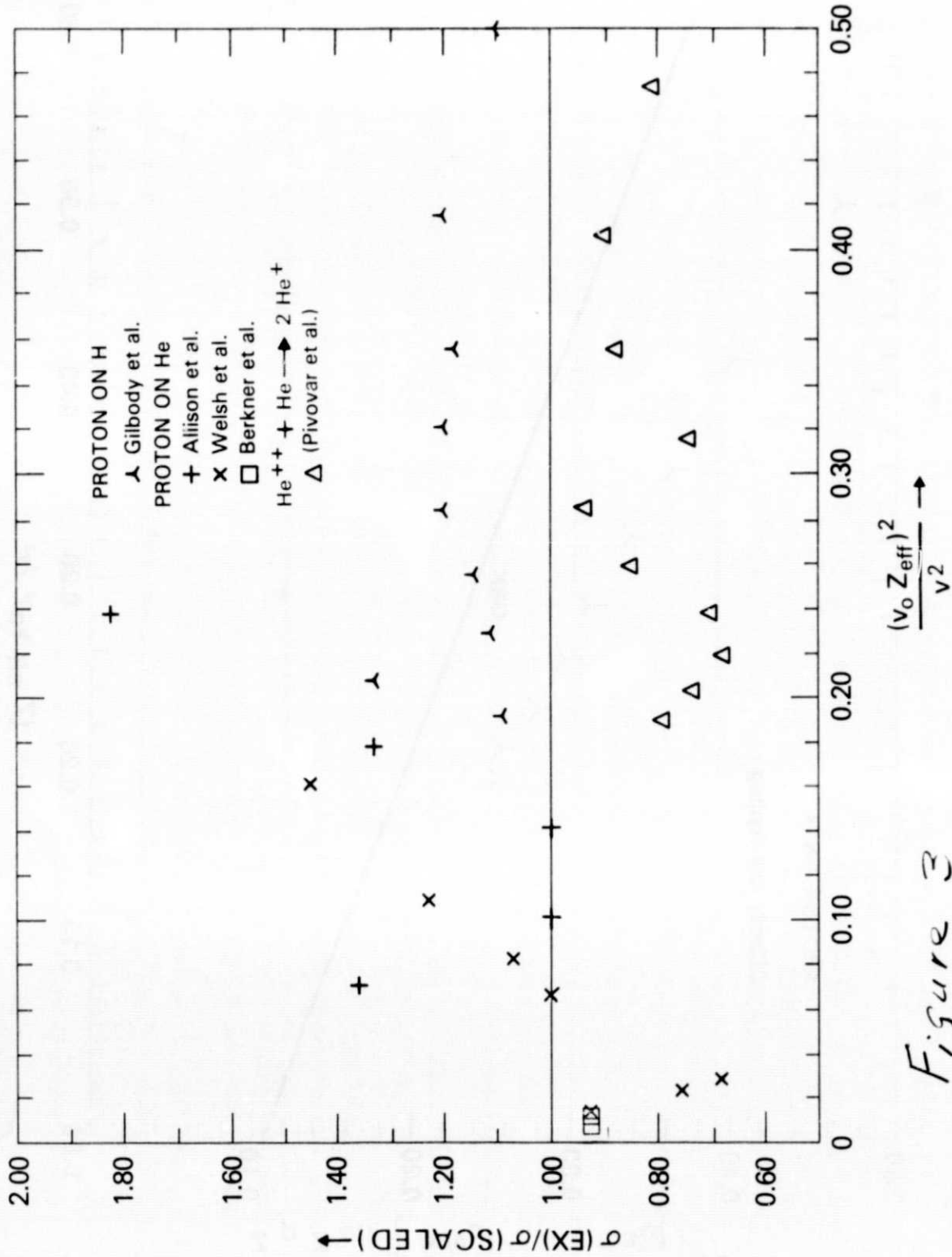


Figure 3

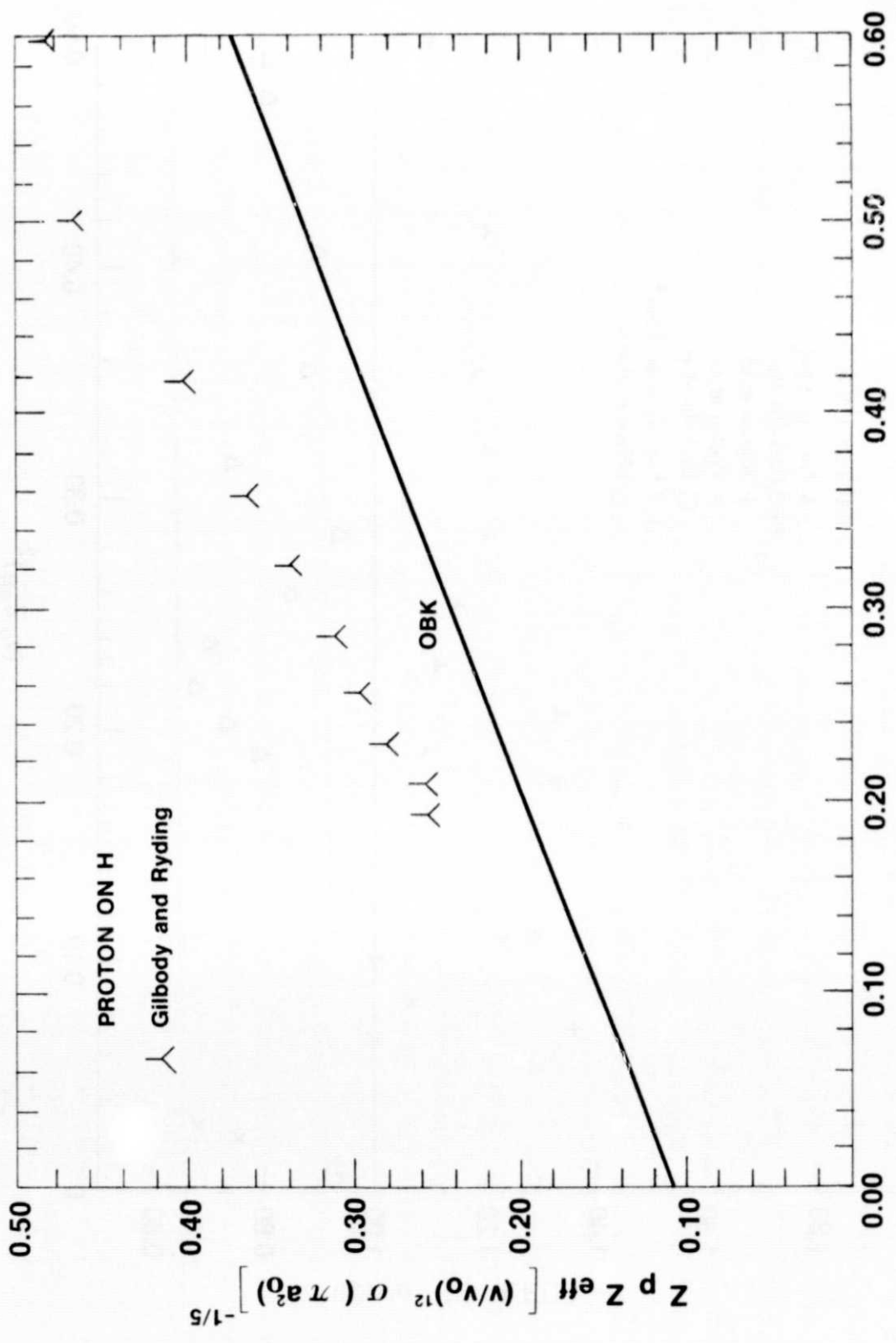


Figure 4

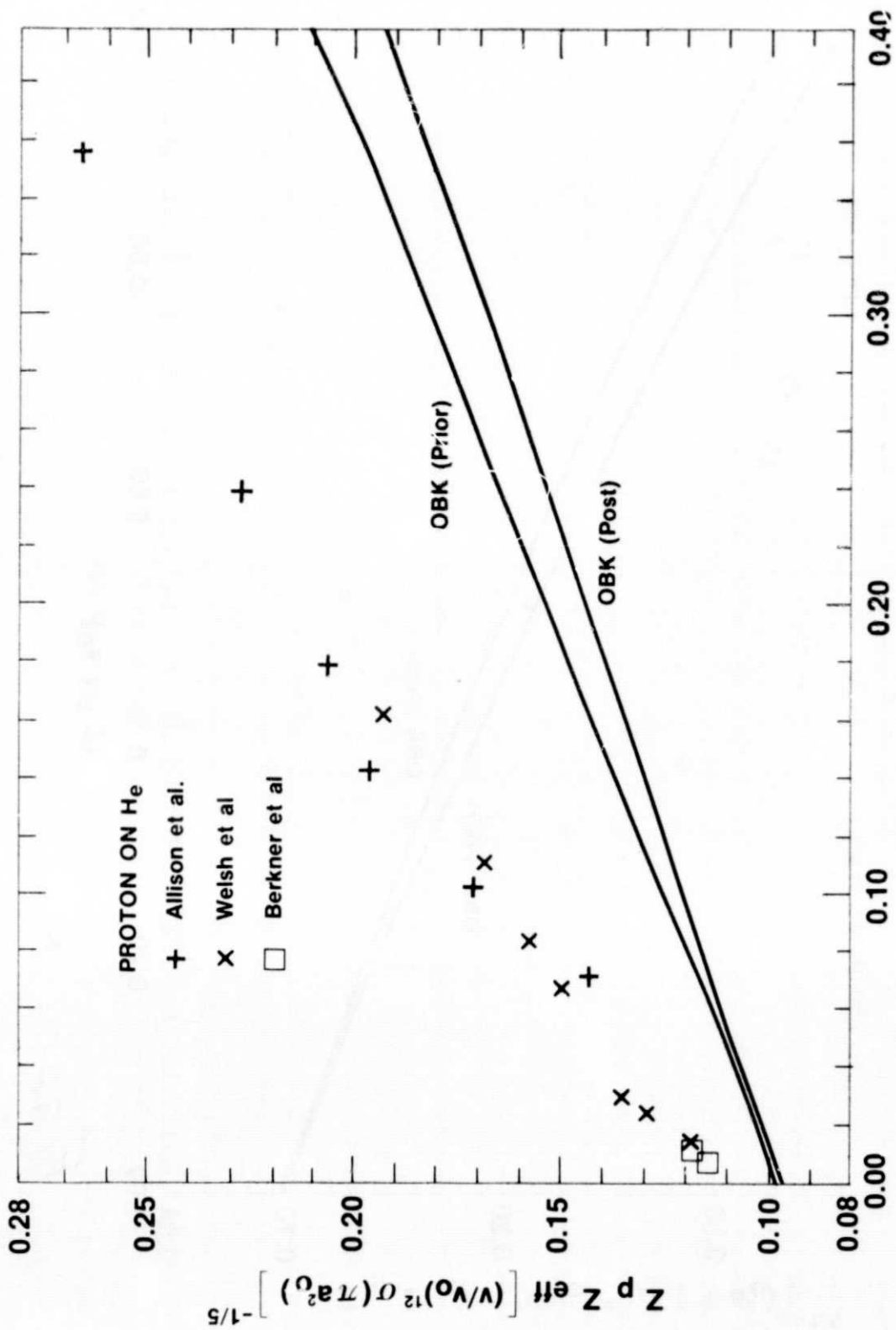


Figure 5

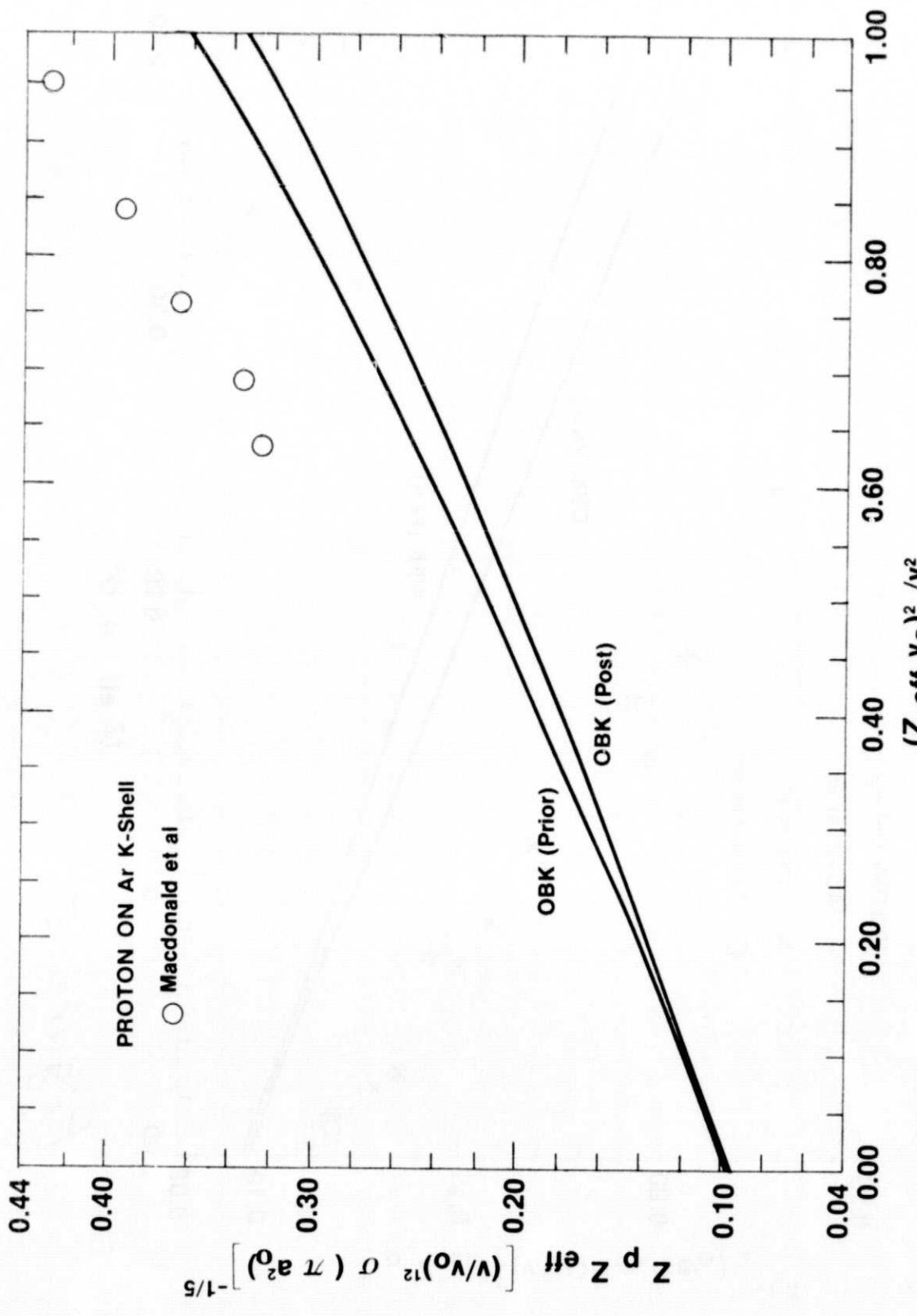


Figure 6

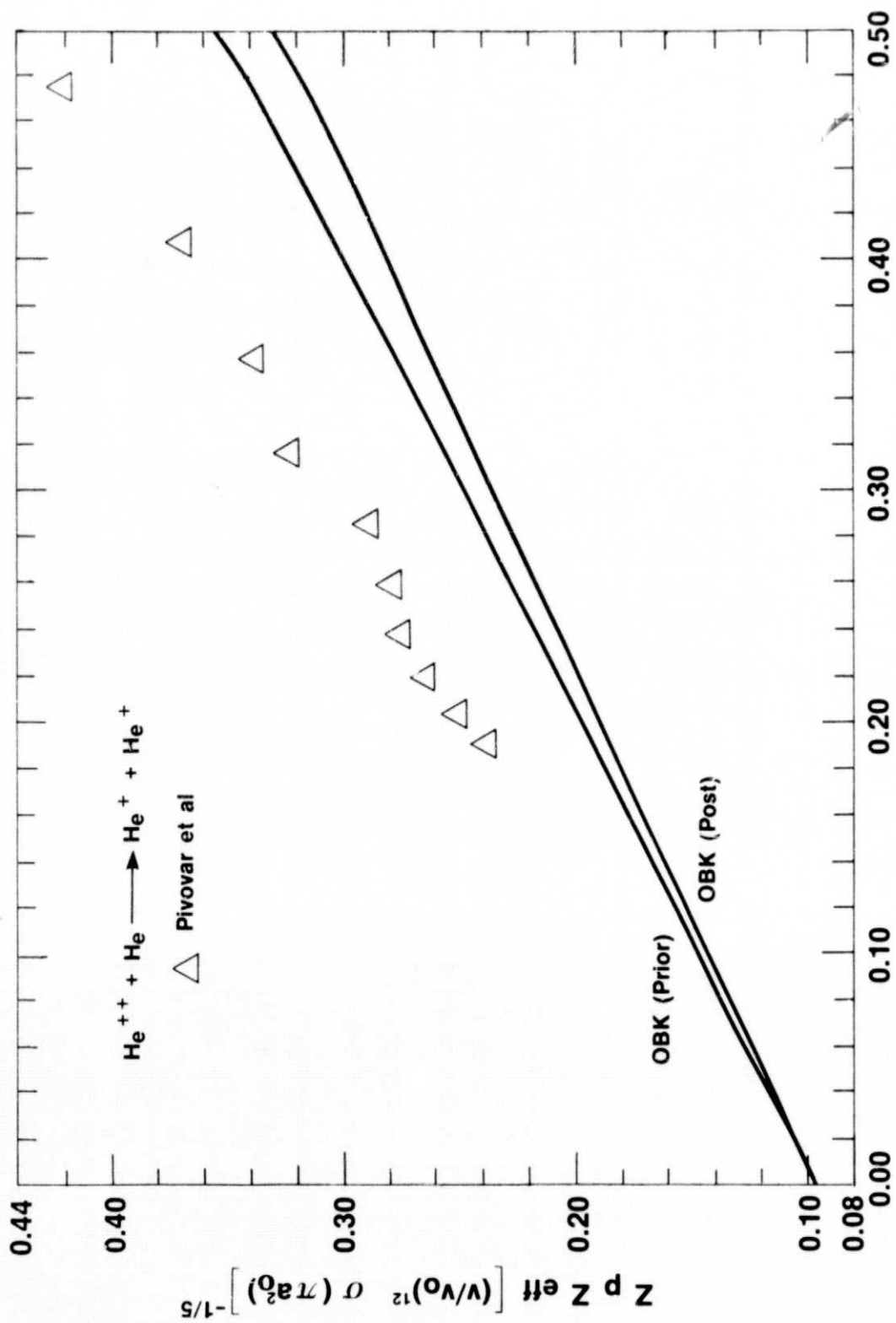


Figure 7